Applied Mathematics & Information Sciences
An International Journal

http://dx.doi.org/10.18576/amis/100441

Stability Analysis for a Constrained Single-Link Flexible Arm using Linear Distributed Parameter Approach

*Liang-Yih Liu**

School of Automation Engineering, Chienkuo Technology University, 50094 Changhua, Taiwan

Received: 25 Nov. 2014, Revised: 8 Jan. 2015, Accepted: 31 Jan. 2015
Published online: 1 Jul. 2016

Abstract: The passivity-based PD force control of a constrained one-link flexible arm is investigated using a linear distributed parameter model. In order to overcome the inherent limitations caused by the non-minimum phase nature of the noncollocation of the joint torque input and the tip contact force output, a new input induced by the measurement of root bending moment and a virtual contact force output generated by a parallel compensator are defined. The transfer function from the new input to the virtual contact force output is passive. A passivity-based PD controller is then designed to accomplish the regulation of the contact force. With the infinite product representations of transcendental functions, exact solutions of the infinite-dimensional system are obtained successfully. This closed loop system has stability robustness to parameter uncertainties and is free spillover problems. Numerical simulations are provided to verify the effectiveness of the proposed approach.

Keywords: Contact force, output redefinition, passive, infinite-dimensional

1 Introduction

In recent years, force control of constrained flexible manipulators has received increasingly attention [1,2,3,4,5,6,7,8,9,10,11,12,13,14,15,16,17,18,19,20,21,22,23]. Application of this research field include space robots used for satellite capturing and large space structure construction, and light weight industrial robots used for assembly, deburring and grinding tasks. The controller design for such force control problems is, however, quite difficult due to the distributed parameter nature of flexible arms and the noncollocation of torque actuation and contact force sensing.

Based on finite-dimensional approximate models, Chiou and Shahinpoor [1,2] studied a single-link and a two-link constrained flexible manipulators, and pointed out that the link flexibility is the main source of dynamic instability of the force controlled systems. Later, Li [3] indicated that an inherent limitation on the achievable bandwidth occurs from the presence of infinitely non-minimum phase zeros. Matsuno et al. [4,5] derived the distributed parameter models and thus proposed hybrid position-force controllers using quasi-static equations. However, the proposed controllers may not guarantee a global stability under possible large initial tracking errors at fast tip speed [5]. Some methods based on a lumped parameter model for a single-link flexible robot were thus developed [6,7,8,9,10] to simplify the dynamics of a flexible arm with the tip forces. On the other hand, it was suitable only for one or two degree of freedom flexible robot [6,7,8,9,10]. Accordingly, a variety of nonlinear hybrid force-position controllers were proposed using nonlinear finite-dimensional dynamic models [11,12,13] for some two and three dimensional constrained flexible robots. However, these proposed methods may not guarantee the stability of the original distributed parameter systems because of spillover problems. Matsuno and Kasai [14] then derived the distributed parameter model for a constrained one-link flexible arm with a concentrated tip mass, a finite-dimensional model for force feedback and compliance control. More recently, Bazaei and Moallem [15] also used distributed parameter model for a constrained flexible beam actuated at the hub. The maximum control bandwidth was obtained by applying the output redefinition. In order to compensate the spillover instability caused by residue modes which are not included in the controller design, an optimal controller with low-pass property and a robust H_∞ controller were proposed in [14,15]. The constrained

* Corresponding author e-mail: lliu@cc.ctu.edu.tw

one-link arm with a symmetric rigid tip body and a nonsymmetric rigid tip body were studied by [16,17]. Bazaei and Moallem [18] improved force control bandwidth of the constrained one-link arm through outputs redefinition. The distributed parameter models were derived in [16,17,18], but finite-dimensional models were still used for controller designs.

As we know that the flexible arm is inherently infinite-dimensional system, the controller design using distributed parameter model becomes more complicated. In order to avoid the spillover from finite-dimensional approximation, the distributed parameter model in [19, 20] was applied to resolve the force control problem for a constrained one-link flexible arm. Unfortunately, the system stability was found only in a sufficient condition [19,20]. Similarly, the stability of the switching collision was also involved into a sufficient condition [21]. Additionally, the exact solutions for the closed-loop system can not be obtained [21]. Recently, the constrained single-link flexible arm studied by [22] with the linear distributed parameter model was used as a starting point. Liu and Lin [23] further extend their work to the constrained one-link flexible arm with internal material damping. However, the passive transfer function was not considered in this study by [23].

To overcome the limitations of above papers, this paper is to show that an exact solution to the above contact force regulation problem can be achieved using a distributed parameter model of the constrained one-link flexible arm. To remove the nonminimum phase obstacle relating the joint torque input and the tip contact force output, a new input induced by the measurement of root bending moment and a virtual contact force output generated by a parallel compensation are defined. It will be shown that the transfer function from the new input to the virtual contact force output is passive. Then, a passivity-based PD control is shown to be able to improve the performance of the infinite dimensional closed loop system. To preserve the exact poles and zeros of the system, the infinite product representations of transfer functions are employed throughout the paper. Numerical simulations are presented to demonstrate the excellent efficacy of the proposed approach.

2 Mathematical model

The constrained one-link flexible arm depicted in figure 1 is a uniform, homogeneous, Euler-Bernoulli beam of length ℓ, mass per unit length ρ, and flexural rigidity EI. The hub is modelled by a single-mass moment of inertia I_h, where the driven torque $\tau(t)$ is applied. The end-effector has a concentrated mass m_p, where the contact force exerted by the smooth rigid constraint surface is $\lambda(t)$. The arm is assumed to move in a horizontal plane so that the gravity can be ignored. Let the X-axis be a fixed frame and x-axis be a floating frame, both coincident with the neutral axis of the beam. The hub angular displacement $\theta(t)$ is defined as the counterclockwise rotation of x-axis with respect to the X-axis. Let $v(x,t)$ be the small transverse deflection of the neutral axis of the beam with respect to the x-axis. Due to the assumption of small transverse deflection, the axial displacement $u(x,t)$ caused by bending foreshortening [24] is negligible. Since $v_\ell(t) = v(\ell,t)$ is assumed small, $\theta(t)$ must also be small. The equations of motion and the corresponding boundary conditions are well-established (e.g. [22,23]).

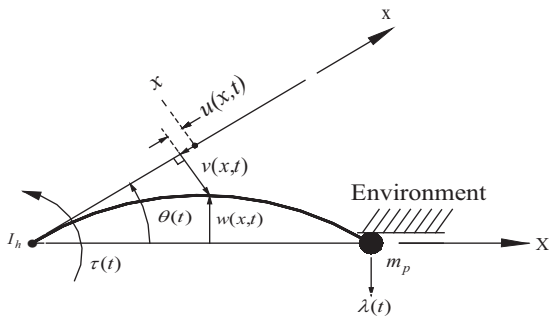

Fig. 1: Schematic of a constrained flexible arm.

$$I_h\ddot{\theta}(t) + \int_0^\ell \rho x\left[x\ddot{\theta}(t) - \ddot{v}(x,t)\right]dx = \tau(t) - \lambda(t)\ell \quad (1)$$

$$\rho\left[-x\ddot{\theta}(t) + \ddot{v}(x,t)\right] + EIv_{xxxx}(x,t) = 0 \quad (2)$$

$$v(0,t) = 0, \quad v(\ell,t) = \ell\theta(t) \quad (3)$$

$$v_x(0,t) = 0 \quad (4)$$

$$v_{xx}(\ell,t) = 0 \quad (5)$$

$$EIv_{xxx}(\ell,t) = -\lambda(t) \quad (6)$$

Substituting Eq. (2) and Eq. (6) into Eq. (1), performing integration by parts and making use of Eq. (5), we obtain an alternative form for Eq. (1) as

$$I_h\ddot{\theta}(t) = \tau(t) - EIv_{xx}(0,t) \quad (7)$$

Note that the exact nonlinear constraint equation is compatible only with the geometric exact nonlinear elastic deflections [25]. In order to use the small deflection assumption consistently, the exact nonlinear constraint equation must be linearized. In an inconsistent formulation [14], Eq. (7) was thus not satisfied. The root bending moment $EIv_{xx}(0,t)$ can be measured by a strain gage sensor [18,20]. Consequently, a new joint input variable $u(t)$ can be expressed as

$$u(t) = \tau(t) - EIv_{xx}(0,t) \quad (8)$$

Then using Eq. (7) reduces to

$$I_h\ddot{\theta}(t) = u(t) \quad (9)$$

Now introduce the new variable $w(x,t)$ such that

$$w(x,t) = x\theta(t) - v(x,t) \tag{10}$$

Then the dynamic equations of the constrained arm (i.e. Eq. (2)–Eq. (7)) become

$$\rho\ddot{w}(x,t) + EIw_{xxxx}(x,t) = 0 \tag{11}$$

$$w(0,t) = 0, \quad w(\ell,t) = 0 \tag{12}$$

$$w_x(0,t) = \theta(t) \tag{13}$$

$$w_{xx}(\ell,t) = 0 \tag{14}$$

$$EIw_{xxx}(\ell,t) = \lambda(t) \tag{15}$$

$$I_h\ddot{\theta}(t) = \tau(t) + EIw_{xx}(0,t) \tag{16}$$

Due to the small deflection assumption, the maximum values of $\lambda(t)$ and $\theta(t)$ must be restricted. This is discussed in the next Section.

3 Validity of small deflection assumption

The objective of this work is to construct a controller which accomplishes the convergence of the contact force from zero to a desired value λ_d without any overshoot. Clearly, the maximum deflection occurs at $x = \ell$ when the steady state is reached. The steady state solution is obtained by solving the time-independent version of Eq. (2)–Eq. (7):

$$v''''(x) = 0 \tag{17}$$

$$v(0) = v'(0) = v''(\ell) = 0, v(\ell) = \ell\theta_d \tag{18}$$

$$EIv'''(\ell) = -\lambda_d, EIv''(0) = \tau_d \tag{19}$$

We obtain

$$\frac{v(\ell)}{\ell} = \theta_d = \frac{\lambda_d\ell^2}{3EI} = \frac{\tau_d\ell}{3EI} \tag{20}$$

Since the small deflection assumption is valid if $\frac{v(\ell)}{\ell} \leq 0.1$, we must set $\lambda_d \leq \frac{0.3EI}{\ell^2}$ and $\theta_d \leq 0.1$ rad.

4 Non-minimum phase transfer function from the input torque to the output contact force

The transfer function can be derived by taking the Laplace transform of Eq. (11)–Eq. (16) with zero initial conditions. Let s be the Laplace transform variable, and define the dimensionless parameters β, ε, and $\hat{s}$

$$\beta^4 = -\frac{\rho\ell^4}{EI}s^2 = -\hat{s}^2, \quad \varepsilon = \frac{I_h}{\rho\ell^3} \tag{21}$$

The solution of Eq. (11) can be written in the Laplace transform domain

$$w(x,\hat{s}) = C_1\cosh\frac{\beta}{\ell}x + C_2\cos\frac{\beta}{\ell}x + C_3\sinh\frac{\beta}{\ell}x + C_4\sin\frac{\beta}{\ell}x \tag{22}$$

where $C_i(\beta)$, $i = 1,2,3,4$ are unknown parameters. Substitution of Eq. (22) into Eq. (9), Eq. (12)–Eq. (16) and solving for C_2, C_3, C_4, θ, λ, τ and u yield

$$C_2 = -C_1 \tag{23}$$

$$C_3 = -\frac{\cosh\beta}{\sinh\beta}C_1, \quad C_4 = \frac{\cos\beta}{\sin\beta}C_1 \tag{24}$$

$$\theta(\hat{s}) = C_1\frac{\beta}{\ell}\cdot\frac{\cos\beta\sinh\beta - \cosh\beta\sin\beta}{\sin\beta\sinh\beta} \tag{25}$$

$$\lambda(\hat{s}) = -C_1EI\frac{\beta^3}{\ell^3}\cdot\frac{\sin\beta + \sinh\beta}{\sin\beta\sinh\beta} \tag{26}$$

$$\tau(\hat{s}) = C_1EI\frac{\beta^2}{\ell^2}\cdot\left[2 + \varepsilon\beta^3\cdot\frac{\cos\beta\sinh\beta - \cosh\beta\sin\beta}{\sin\beta\sinh\beta}\right] \tag{27}$$

$$u(\hat{s}) = -C_1EI\frac{\beta^5}{\ell^2}\varepsilon\cdot\frac{\cos\beta\sinh\beta - \cosh\beta\sin\beta}{\sin\beta\sinh\beta} \tag{28}$$

After algebraic manipulations, one obtains

$$\frac{\lambda(\hat{s})}{\tau(\hat{s})} = G_{\lambda\tau}(\hat{s}) = \frac{\beta}{\ell}\cdot\frac{\sinh\beta + \sin\beta}{2\sinh\beta\sin\beta - \varepsilon\beta^3(\cosh\beta\sin\beta - \sinh\beta\cos\beta)} \tag{29}$$

By applying the infinite product expansions of transcendental functions (see A1 to A3 of the Appendix), Eq. (29) can be rewritten as

$$G_{\lambda\tau}(\hat{s}) = \frac{1}{\ell}\cdot\frac{\prod_{n=1}^{\infty}\left(1 - \frac{\hat{s}^2}{\omega_{zn}^2}\right)}{\prod_{n=1}^{\infty}\left(1 + \frac{\hat{s}^2}{n^4\pi^4}\right) + \frac{\varepsilon\hat{s}^2}{3}\prod_{n=1}^{\infty}\left(1 + \frac{\hat{s}^2}{\omega_{\beta n}^2}\right)} \tag{30}$$

where $\pm jn^2\pi^2$ and $\pm j\omega_{\beta n}$ are the familiar pinned-pinned and clamped-pinned bending vibration modes, respectively. The poles of $G_{\lambda\tau}(\hat{s})$ are the roots of the equation

$$\frac{\varepsilon}{3}\cdot\frac{\hat{s}^2\prod_{n=1}^{\infty}\left(1 + \frac{\hat{s}^2}{\omega_{\beta n}^2}\right)}{\prod_{n=1}^{\infty}\left(1 + \frac{\hat{s}^2}{n^4\pi^4}\right)} = -1 \tag{31}$$

Note that with $\omega_{\beta 0}=0$, the interlacing property $\omega_{\beta,n-1}<n^2\pi^2<\omega_{\beta n}$ holds for $n=1,2\cdots$ (see A2 and A3 of the Appendix). Using the root locus method, it can be easily shown that the poles of $G_{\lambda\tau}(\hat{s})$ moves along the imaginary $\hat{s}$-axis from $\pm jn^2\pi^2$ to $\pm j\omega_{\beta n}$ as ε increases from 0 to ∞. Let the roots of Eq. (31) (for a fixed value of ε) be $\hat{s}=\pm j\omega_{\theta n}$, $n=1,2\cdots$, where $\omega_{\theta n}<\omega_{\theta,n+1}$. Then Eq. (30) becomes

$$G_{\lambda\tau}(\hat{s})=\frac{1}{\ell}\cdot\frac{\prod_{n=1}^{N}\left(1-\frac{\hat{s}^2}{\omega_{zn}^2}\right)}{\prod_{n=1}^{N+1}\left(1+\frac{\hat{s}^2}{\omega_{\theta n}^2}\right)},\quad N\to\infty \tag{32}$$

The numerical values of $\omega_{\theta n}(\varepsilon)$ can be computed using $\omega_{\theta n}=\beta_n^2$, where $\beta_n(\varepsilon)$ are the positive real roots of the denominator of Eq. (29), namely

$$2\sinh\beta\sin\beta-\varepsilon\beta^3(\cosh\beta\sin\beta-\sinh\beta\cos\beta)=0 \tag{33}$$

The values obtained by selected $\omega_{\theta n}$ are listed in Table 1.

It is well established [3,26] that the existence of non-minimum phase zeros imposes fundamental limitations in the achievable performance of the closed-loop system. To alleviate the non-minimum phase problem, the real zeros of $G_{\lambda\tau}(\hat{s})$ can be replaced by the zeros on the imaginary $\hat{s}$-axis using the method of redefinition of output [27]. With the new output, the transfer function is marginal minimum phase but not necessarily passive. Fortunately, the poles of $G_{\lambda\tau}(\hat{s})$ can be made to move along the imaginary $\hat{s}$-axis by using an appropriate feedback. Combining the feedback and the output redefinition, it is possible to find a new transfer function which satisfies the so-called the interlacing property. A transfer function with a simple pole at the origin is said to satisfy the interlacing property if all its poles and zeros lie on the imaginary $\hat{s}$-axis, are distinct and alternate each other. Such transfer functions are known as passive transfer functions [28].

5 Achieving passivity by Parallel Compensation

It is well known that for non-minimum phase systems, perfect asymptotic tracking of output trajectories with internal stability cannot be achieved. To alleviate the non-minimum phase problem, the right half-plane zeros can be replaced by the left half-plane zeros by the method of redefinition of output. Define a new virtual contact force $f(t,k)$ such that

$$\begin{aligned}G_{fu}(\hat{s},k)&=\frac{f(\hat{s},k)}{u(\hat{s})}\\&=\frac{1}{\ell\varepsilon\beta^2}\cdot\frac{k(\sin\beta+\sinh\beta)+(1-k)\beta(1+\cosh\beta\cos\beta)}{\cos\beta\sinh\beta-\cosh\beta\sin\beta}\end{aligned} \tag{34}$$

where k is a real constant and $k\le 0.758$ that was shown in [27]. One can write

$$\begin{aligned}&k(\sin\beta+\sinh\beta)+(1-k)\beta(1+\cosh\beta\cos\beta)\\&\quad=2\beta\prod_{n=1}^{\infty}\left(1+\frac{\hat{s}^2}{\omega_{\alpha n}^2}\right)\end{aligned} \tag{35}$$

The numerical values can be computed using $\omega_{\alpha n}=\beta_n^2$, where $\beta_n(k)$, $n=1,2,\cdots$ is the real positive roots of the numerator of Eq. (34). Selected $\omega_{\alpha n}$ values are listed in Table 1. Thus, one has a minimum phase stable transfer function

$$G_{fu}(\hat{s},k)=\frac{3}{\ell\varepsilon}\cdot\frac{\prod_{n=1}^{\infty}\left(1+\frac{\hat{s}^2}{\omega_{\alpha n}^2}\right)}{\hat{s}^2\prod_{n=1}^{\infty}\left(1+\frac{\hat{s}^2}{\omega_{\beta n}^2}\right)} \tag{36}$$

Note that the above redefinition of output is equivalent to the parallel compensation [29] as shown in figure 2. It can be shown that the parallel compensator $T(\hat{s},k)$ has the form

$$\begin{aligned}T(\hat{s},k)&=\frac{(1-k)}{\ell\varepsilon\beta^2}\cdot\frac{\beta(1+\cosh\beta\cos\beta)-(\sin\beta+\sinh\beta)}{\cos\beta\sinh\beta-\cosh\beta\sin\beta}\\&=\frac{11(1-k)}{40\ell\varepsilon}\cdot\frac{\prod_{n=1}^{\infty}\left(1+\frac{\hat{s}^2}{\omega_{\delta n}^2}\right)}{\prod_{n=1}^{\infty}\left(1+\frac{\hat{s}^2}{\omega_{\beta n}^2}\right)}\end{aligned} \tag{37}$$

where $\omega_{\delta n}=\beta_n^2$ and $\beta_n(k)$, $n=1,2\cdots$ are the real positive roots of the equation

$$\beta(1+\cosh\beta\cos\beta)-(\sin\beta+\sinh\beta)=0 \tag{38}$$

Selected values of $\omega_{\delta n}$ are computed and listed in Table 1.

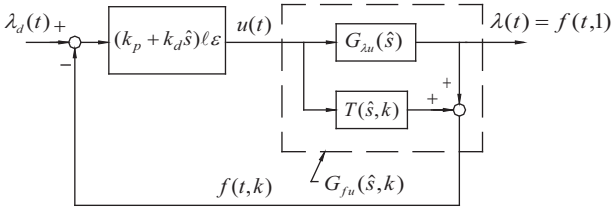

Fig. 2: Passive PD control of parallel compensated system.

Using Eq. (25)–Eq. (28) and application of infinite product representation of transcendental functions given in the Appendix, it is easy to verify that

$$\begin{aligned}G_{\lambda u}(\hat{s})=\frac{\lambda(\hat{s})}{u(\hat{s})}&=\frac{1}{\ell\varepsilon\beta^2}\cdot\frac{\sinh\beta+\sin\beta}{\cos\beta\sinh\beta-\cosh\beta\sin\beta}\\&=\frac{3}{\ell\varepsilon}\cdot\frac{\prod_{n=1}^{\infty}\left(1-\frac{\hat{s}^2}{\omega_{zn}^2}\right)}{\hat{s}^2\prod_{n=1}^{\infty}\left(1+\frac{\hat{s}^2}{\omega_{\beta n}^2}\right)}\end{aligned} \tag{39}$$

Table 1: Values of roots of associated transcendental equations

n	$\omega_{\alpha n}(k=0.7)$	$\omega_{\beta n}$	$\omega_{\delta n}$	$\omega_{\theta n}(\varepsilon = 3.387\times 10^{-2})$
0		0 0		
1	2.847^2	3.927^2	4.900^2	2.686^2
2	4.082^2	7.069^2	7.725^2	4.410^2
3	8.145^2	10.210^2	11.086^2	7.156^2
4	10.777^2	13.352^2	14.066^2	10.238^2
5	14.301^2	16.493^2	17.336^2	13.364^2
6	17.142^2	19.635^2	20.371^2	16.500^2
$\vdots$	$(n=odd)$ $\vdots$ $(n=even)$	$\vdots$	$(n=odd)$ $\vdots$ $(n=even)$	$\vdots$
	$\left[(n-\frac{1}{2})\pi+\frac{7}{3(n-\frac{1}{2})\pi}\right]^2$	$\left[(n+\frac{1}{2})\pi+\frac{1}{(n+\frac{1}{2})\pi}\right]^2$		$\left[(n-\frac{3}{4})\pi+\frac{29.5}{(n-\frac{3}{4})^3\pi^3}\right]^2$
	$\left[(n-\frac{1}{2})\pi-\frac{7}{3(n-\frac{1}{2})\pi}\right]^2$	$(n+\frac{1}{4})^2\pi^2$	$\left[(n+\frac{1}{2})\pi-\frac{1}{(n+\frac{1}{2})\pi}\right]^2$	

$$G_{\theta u}(\hat{s}) = \frac{\theta(\hat{s})}{u(\hat{s})} = \frac{\ell}{\varepsilon EI}\cdot\frac{1}{\hat{s}^2} \tag{40}$$

$$G_{\tau u}(\hat{s}) = \frac{\tau(\hat{s})}{u(\hat{s})}$$
$$= \frac{1}{\varepsilon\beta^3}\cdot\frac{2\sinh\beta\sin\beta-\varepsilon\beta^3(\cosh\beta\sin\beta-\sinh\beta\cos\beta)}{\cos\beta\sinh\beta-\cosh\beta\sin\beta}$$
$$= \frac{3}{\varepsilon\hat{s}^2}\cdot\frac{\prod_{n=1}^{\infty}\left(1+\frac{\hat{s}^2}{\omega_{\theta n}^2}\right)}{\prod_{n=1}^{\infty}\left(1+\frac{\hat{s}^2}{\omega_{\beta n}^2}\right)} \tag{41}$$

6 Proof of passivity of $\hat{s}G_{fu}(\hat{s})$

Let $\hat{s}G_{fu}(\hat{s})$ be express as

$$\hat{s}G_{fu}(\hat{s}) = \frac{3}{\ell\varepsilon}\cdot\frac{\prod_{n=1}^{N}\left(1+\frac{\hat{s}^2}{\omega_{\alpha n}^2}\right)}{\hat{s}\prod_{n=1}^{N}\left(1+\frac{\hat{s}^2}{\omega_{\beta n}^2}\right)} = \frac{A_0}{\hat{s}}+\sum_{i=1}^{N}\frac{A_i\hat{s}}{\hat{s}^2+\omega_{\beta n}^2} \tag{42}$$

where by assumption $N\to\infty$, $0<\omega_{\alpha 1}<\omega_{\alpha 2}<\cdots<\omega_{\alpha N}<\cdots$, and $0<\omega_{\beta 1}<\omega_{\beta 2}<\cdots<\omega_{\beta N}<\cdots$. It is easy to show that $A_0=\frac{3}{\ell\varepsilon}$ and

$$A_i = -\frac{A_0}{\omega_{\alpha i}^2}\prod_{n=1}^{N}\left(\frac{\omega_{\beta n}}{\omega_{\alpha n}}\right)^2\frac{\prod_{n=1}^{N}\left(\omega_{\alpha n}^2-\omega_{\beta i}^2\right)}{\prod_{\substack{n=1\\ n\neq i}}^{N}\left(\omega_{\beta n}^2-\omega_{\beta i}^2\right)} \tag{43}$$

for $i=1,2,\cdots,N$. Note that if $A_0>0$ and $A_i>0$ for $i=1,2,\cdots(N\to\infty)$, then $\hat{s}G_{fu}(\hat{s})$ is a passive transfer function since it is the sum of passive transfer functions (see Eq. (42)). We now proceed to prove the assertion by induction that if $A_i>0, i=1,2,\cdots(N\to\infty)$, then the interlacing property holds for $\hat{s}G_{fu}(\hat{s})$. Using the second and third columns of Table 1 and referring to Eq. (42), it can be easily shown that (i) for $N=1$, $A_1>0$ implies $\omega_{\alpha 1}<\omega_{\beta 1}$, and (ii) for $N=2$ and $\omega_{\alpha 1}<\omega_{\beta 1}$, $A_1>0$ implies $\omega_{\beta 1}<\omega_{\alpha 2}$ and $A_2>0$ implies $\omega_{\alpha 2}<\omega_{\beta 2}$. Assume that for each positive integer $N, A_i>0$, $i=1,2,\cdots,N$ imply $0<\omega_{\alpha 1}<\omega_{\beta 1}<\omega_{\alpha 2}<\omega_{\beta 2}<\cdots<\omega_{\alpha N}<\omega_{\beta N}$. Then for the positive integer $N+1$, it can be shown using Eq. (43) that $A_i>0$, $i=1,2,\cdots,N$ imply $\omega_{\beta N}<\omega_{\alpha,N+1}$ and $A_{N+1}>0$ implies $\omega_{\alpha,N+1}<\omega_{\beta,N+1}$. This proves the above assertion for all positive integers N. One concludes that $\hat{s}G_{fu}(\hat{s})$ satisfies the interlacing property. Therefore, $\hat{s}G_{fu}(\hat{s})$ is a passive transfer function. It may be remarked at this point that if $k\neq 0.7$, then the zeros of $G_{fu}(\hat{s})$ must be computed numerically. It was found that $\hat{s}G_{fu}(\hat{s})$ is passive for $k<0.730$ (the restriction that $k\neq 0.730$ is due to the cancellation of first pole $\pm j\omega_{\beta 1}$ and the second

zero $\pm j\omega_{\alpha 2}$ at the $k = 0.730$, the details are rather involved and thus omitted). It is known [28,30] that the passivity property of $\hat{s}G_{fu}(\hat{s})$ permits the design of a large family of stabilizing controllers. In what follows, only a simple feedforward PD controller will be considered for the regulation of the contact force $\lambda(t)$.

7 Passivity-based PD controller

For the control structure as shown in figure 2, the objective is to make $\lambda(t)$ to track asymptotically a desired contact force trajectory $\lambda_d(t)$ using a PD control law

$$u(\hat{s},k) = -(k_p + k_d\hat{s})\ell\varepsilon\,[f(\hat{s},k) - \lambda_d(\hat{s})] \qquad (44)$$

where $\lambda_d(\hat{s})$ is the Laplace transform of the desired contact force trajectory, k_p and k_d are positive design constants, and $k < 0.730$. One obtains

$$f(\hat{s},k) = \frac{(k_p + k_d\hat{s})\ell\varepsilon G_{fu}(\hat{s},k)}{1 + (k_p + k_d\hat{s})\ell\varepsilon G_{fu}(\hat{s},k)}\lambda_d(\hat{s}) \qquad (45)$$

Combining Eq. (44)–Eq. (45) gives

$$u(\hat{s},k) = \frac{(k_p + k_d\hat{s})\ell\varepsilon}{1 + (k_p + k_d\hat{s})\ell\varepsilon G_{fu}(\hat{s},k)}\lambda_d(\hat{s}) \qquad (46)$$

The poles of the closed-loop system are given by the roots of the characteristic equation

$$1 + (k_p + k_d\hat{s})\ell\varepsilon G_{fu}(\hat{s},k) = 0 \qquad (47)$$

With $G_{fu}(\hat{s},k)$ given by Eq. (36), Eq. (47) becomes

$$3(k_p + k_d\hat{s}) \cdot \frac{\prod_{n=1}^{\infty}\left(1 + \frac{\hat{s}^2}{\omega_{\alpha n}^2}\right)}{\hat{s}^2\prod_{n=1}^{\infty}\left(1 + \frac{\hat{s}^2}{\omega_{\beta n}^2}\right)} = -1 \qquad (48)$$

Clearly, the effect of P-control alone is merely to move all the closed-loop poles along the imaginary $\hat{s}$-axis from $\hat{s} = \pm j\omega_{\beta,n-1}$ (set $\omega_{\beta 0} = 0$) to $\hat{s} = \pm j\omega_{\alpha n}$, $n = 1,2,\cdots$ as k_p varies from 0 to ∞ (see figure 3a). With $k_p = k_p^*$, Eq. (48) can be rewritten as

$$\frac{k_d}{k_p^*} \cdot \frac{\hat{s}\prod_{n=1}^{N}\left(1 + \frac{\hat{s}^2}{\omega_{\alpha n}^2}\right)}{\prod_{n=1}^{N+1}\left(1 + \frac{\hat{s}^2}{\omega_{\delta n}^2}\right)} = -1, N \to \infty \qquad (49)$$

It can be verified (see figure 3b) using a simple root locus plot that the D-control suffices to stabilize the closed-loop system for all $0 < k_p^* < \infty$ and $0 < k_d < \infty$.

Let the roots of Eq. (48) be written as

$$\hat{s}_n = \sqrt{\frac{\rho\ell^4}{EI}}s_n = -\zeta_n\Omega_n \pm j\Omega_n\sqrt{1-\zeta_n^2}, n = 1,2,\cdots \qquad (50)$$

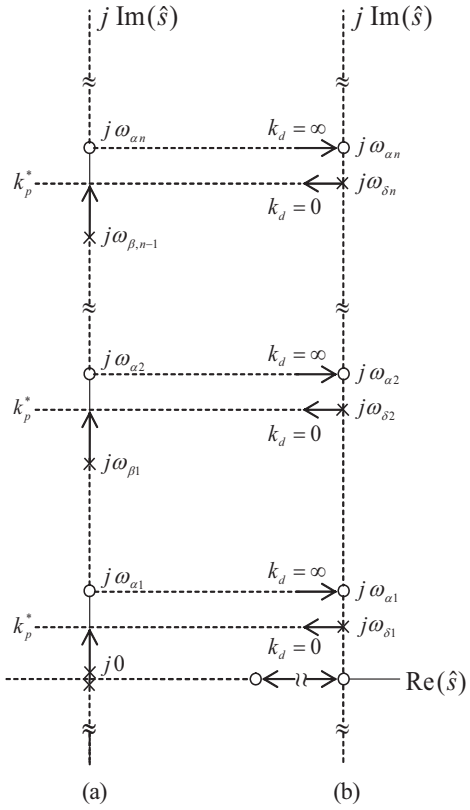

Fig. 3: Effects of P-control and D-control : (a) $k_d = 0, 0 \le k_p < \infty$; (b) $k_p = k_p^*, 0 \le k_d < \infty$.

where $\Omega_n(\Omega_n < \Omega_{n+1})$ and ζ_n are the natural frequency and damping ratio of the*n-th* closed-loop pole. Then one may write Eq. (48) as

$$\begin{aligned} &3(k_p + k_d\hat{s})\prod_{n=1}^{N}\left(1 + \frac{\hat{s}^2}{\omega_{\alpha n}^2}\right) + \hat{s}^2\prod_{n=1}^{N}\left(1 + \frac{\hat{s}^2}{\omega_{\beta n}^2}\right) \\ &= 3k_p\prod_{n=1}^{N+1}\left(1 + 2\zeta_n\frac{\hat{s}}{\Omega_n} + \frac{\hat{s}^2}{\Omega_n^2}\right), N \to \infty \end{aligned} \qquad (51)$$

Using Eq. (46) for $u(\hat{s},k)$ and $G_{fu}(\hat{s},k)$, $G_{\lambda u}(\hat{s})$, $G_{v_{xx}u}(\hat{s})$, $G_{\theta u}(\hat{s})$, $G_{\tau u}(\hat{s})$ given by Eq. (36), Eq. (39)–Eq. (41), the closed-loop responses of some relevant variables can be computed as follows.

$$\begin{aligned} &f(\hat{s},k) = G_{fu}(\hat{s},k)u(\hat{s},k) \\ &= \left(1 + \frac{k_d}{k_p}\hat{s}\right) \cdot \frac{\prod_{n=1}^{N}\left(1 + \frac{\hat{s}^2}{\omega_{\alpha n}^2}\right)}{\prod_{n=1}^{N+1}\left(1 + 2\zeta_n\frac{\hat{s}}{\Omega_n} + \frac{\hat{s}^2}{\Omega_n^2}\right)}\lambda_d(\hat{s}), \\ &N \to \infty \\ &\lambda(\hat{s}) = G_{\lambda u}(\hat{s})u(\hat{s},k) \end{aligned} \qquad (52)$$

$$= \left(1+\frac{k_d}{k_p}\hat{s}\right)\cdot\frac{\prod_{n=1}^{N}\left(1-\frac{\hat{s}^2}{\omega_{zn}^2}\right)}{\prod_{n=1}^{N+1}\left(1+2\zeta_n\frac{\hat{s}}{\Omega_n}+\frac{\hat{s}^2}{\Omega_n^2}\right)}\lambda_d(\hat{s}), \quad (53)$$

$N\to\infty$

$\theta(\hat{s}) = G_{\theta u}(\hat{s})u(\hat{s},k)$

$$= \left(1+\frac{k_d}{k_p}\hat{s}\right)\cdot\frac{\ell^2\prod_{n=1}^{N}\left(1+\frac{\hat{s}^2}{\omega_{\beta n}^2}\right)}{3EI\prod_{n=1}^{N+1}\left(1+2\zeta_n\frac{\hat{s}}{\Omega_n}+\frac{\hat{s}^2}{\Omega_n^2}\right)}\lambda_d(\hat{s}),$$

$N\to\infty$ (54)

$\tau(\hat{s}) = G_{\tau u}(\hat{s})u(\hat{s},k)$

$$= \left(1+\frac{k_d}{k_p}\hat{s}\right)\cdot\frac{\ell\prod_{n=1}^{N}\left(1+\frac{\hat{s}^2}{\omega_{\theta n}^2}\right)}{\prod_{n=1}^{N+1}\left(1+2\zeta_n\frac{\hat{s}}{\Omega_n}+\frac{\hat{s}^2}{\Omega_n^2}\right)}\lambda_d(\hat{s}), \quad (55)$$

$N\to\infty$

Note that the above results are exact closed-loop solutions of the infinite-dimensional force control system. To perform the inverse Laplace transform, $\hat{s}$ can be replaced by $\sqrt{\frac{\rho\ell^4}{EI}}s$. The closed-loop time responses can be computed within an arbitrary degree of accuracy by taking N as large as required. In order to find the exact values (to the extent of numerical accuracy) of the closed-loop poles (i.e. the roots of Eq. (47)), $G_{fu}(\hat{s},k)$ given by Eq. (34) must be used. Using either of $\beta = \pm\sqrt{j\hat{s}}$ and $\pm j\sqrt{j\hat{s}}$, Eq. (47) becomes

$$(k_p+k_d\hat{s})[k(\sin\sqrt{j\hat{s}}+\sinh\sqrt{j\hat{s}})+(1-k)\sqrt{j\hat{s}}(1+\cosh\sqrt{j\hat{s}}\cos\sqrt{j\hat{s}})]+j\hat{s}(\cos\sqrt{j\hat{s}}\sinh\sqrt{j\hat{s}}-\cosh\sqrt{j\hat{s}}\sin\sqrt{j\hat{s}}) = 0 \quad (56)$$

This equation can be solved numerically to yield Ω_n and ζ_n, $n = 1,2\cdots$. The control structure of figure 2 can be converted to the basic feedback loop as shown in figure 4.

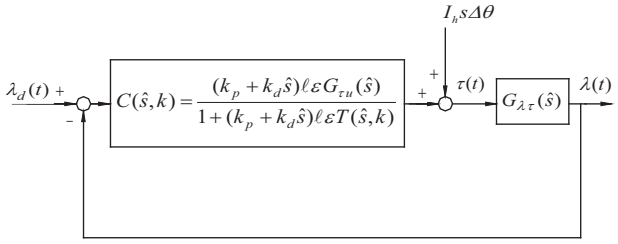

Fig. 4: Overall closed-loop system in basic feedback loop.

Using Eq. (37) and Eq. (41), it is not difficult to show that the transfer function of the compensator is

$$C(\hat{s}) = \frac{(k_p+k_d\hat{s})\ell[2\beta^{-2}\sinh\beta\sin\beta+\varepsilon\beta K(\beta)]}{\beta K(\beta)+(k_p+k_d\hat{s})(1-k)[(1+\cosh\beta\cos\beta)-\beta^{-1}(\sinh\beta+\sin\beta)]}$$

$$= \left(1+\frac{k_d}{k_p}\hat{s}\right)\cdot\frac{\ell\prod_{n=1}^{M}\left(1+\frac{\hat{s}^2}{\omega_{\theta n}^2}\right)}{(1-k)\prod_{n=1}^{N}\left(1+2\zeta_{cn}\frac{\hat{s}}{\omega_{cn}}+\frac{\hat{s}^2}{\omega_{cn}^2}\right)}, \quad (57)$$

$M,N\to\infty$

where $K(\beta) = \sinh\beta\cos\beta-\cosh\beta\sin\beta, \hat{s} = -\zeta_{cn}\omega_{cn}\pm j\omega_{cn}\sqrt{1-\zeta_{cn}^2}$, $n = 1,2\cdots$, are the poles of $C(\hat{s})$ determined by the roots of denominator of Eq. (57) using either of $\beta = \pm\sqrt{j\hat{s}}$ and $\pm j\sqrt{j\hat{s}}$. Since the compensator is infinite dimensional, its implementation is not practically feasible. However, due to the finite bandwidth of the physical sensor and actuator, a finite dimensional compensator $C_{red}(\hat{s})$ can be obtained by truncating the high frequency terms of the infinite product part of $C(\hat{s})$ for some properly chosen positive integers N and M. Let N and M be selected such that $C_{red}(\hat{s})$ has the same poles, zeros, and gain as $C(\hat{s})$ within the frequency band of interest containing the crossover region of $C(\hat{s})G_{\lambda\tau}(\hat{s})$. Then the reduced order compensator $C_{red}(\hat{s})$ is able to maintain desirable closed loop stability and performance. To ensure that the closed loop system is robustly stable with respect to the measurement noise, one may keep fewer zeros than poles of $C_{red}(\hat{s})$. This added high frequency roll-off of $C_{red}(\hat{s})G_{\lambda\tau}(\hat{s})$ further diminishes the effects of the high frequency modes of $G_{\lambda\tau}(\hat{s})$. Finally, since $C_{red}(\hat{s})$ and $G_{\lambda\tau}(\hat{s})$ are proper, $C_{red}(\hat{s})G_{\lambda\tau}(\hat{s})$ has no pole-zero cancellation in $Re(\hat{s})\geq 0$, and $1+C_{red}(\hat{s})G_{\lambda\tau}(\hat{s}) = 0$ has no zeros in $Re(\hat{s})\geq 0$, the closed loop system is internally stable [31].

8 Simulation

The effectiveness of the proposed control approach is evaluated here through numerical simulation using the parameters of an experimental apparatus described in [14]. These parameters are: $\rho = 0.405$ kg/m, $E = 2.06\times10^{11}$ N/m^2, $\ell = 0.9$ m, $I = 1.41\times10^{-11}$ m^4, $I_h = 0.01$ kg-m^2 ($\varepsilon = 3.387\times10^{-2}$). The values of $\omega_{\alpha n}$, $\omega_{\beta n}$, $\omega_{\theta n}$ and $\omega_{\delta n}$ can be found in the Appendix and Table 1. The virtual contact force parameter and controller gain that resulted in good performance were selected as $k = 0.7, k_p = 3.054$, and $k_d = 1.847$. The desired contact force trajectory was selected as

$$\lambda_d(t) = 1-6e^{-5t}+5e^{-6t} \quad (58)$$

which results in $\lim_{t\to\infty}\lambda(t) = \lim_{t\to\infty}f(t,0.7) = 1$ N, $\lim_{t\to\infty}\tau(t) = 0.9$ N-m, and $\lim_{t\to\infty}\theta(t) = 9.296\times10^{-2}$ rad. The first six pairs of closed-loop poles computed from Eq. (56) are $\hat{s} = -16.381, -16.381, -16.381, -10302.250, -1.983\pm$

$j52.906, -14.594 \pm j216.364, -8.762 \pm j382.309$, and $-11.146 \pm j675.169$. The simulation results which are hardly discernible for $N = M \geq 4$ are shown in figure 5. For example, $|\lambda_{N+1}(t) - \lambda_N(t)|/|\lambda_N(t)| \leq 1.375 \times 10^{-5}$, $|\tau_{N+1}(t) - \tau_N(t)|/\tau_N(t) \leq 7.453 \times 10^{-4}$, and $|\theta_{N+1}(t) - \theta_N(t)|/|\theta_N(t)| \leq 2.631 \times 10^{-5}$.

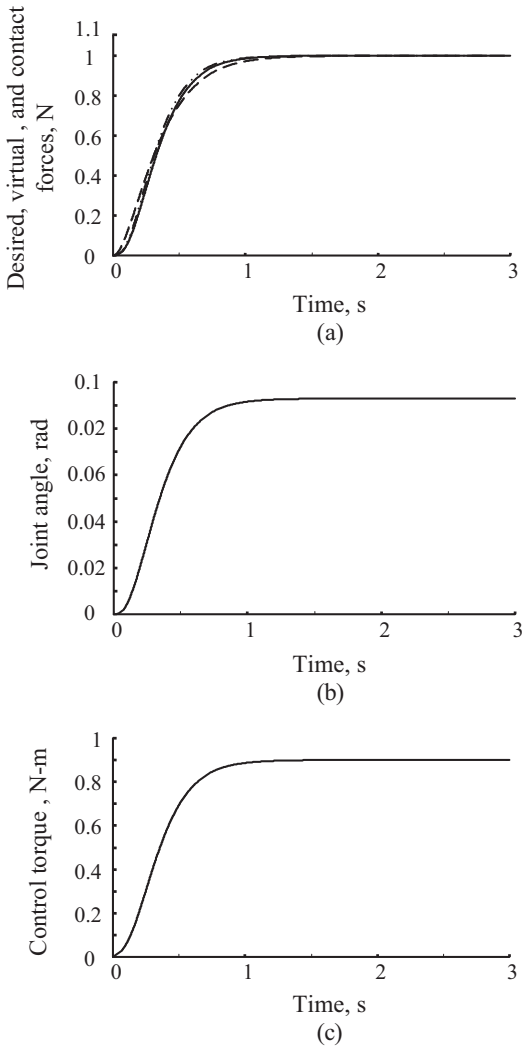

Fig. 5: Contact force regulation (a) $\lambda(t)$ – – –, $f(t,0.7)$ ——, $\lambda_d(t)$ – · · –; (b) $\theta(t)$; (c) $\tau(t)$.

Let $w(x,t) := x\theta(t) - v(x,t)$, and $w_d(x) := x\theta_d - v_d(x)$. Assume that the flexible link remains in the steady state (i.e. $\Delta w(x) := w(x,0) - w_d(x) = 0$), but there is an initial joint angular displacement (i.e. $\Delta\theta := \theta(0) - \theta_d \neq 0$, and $\Delta\dot{\theta} := \lim_{t\to 0}\dot{\theta}(t) = 0$). Since the Laplace transform of Eq. (14) yield $I_h[s^2\Delta\theta(s) - s\Delta\theta(0) - \Delta\dot{\theta}(0)] = u(s)$ the initial joint angular displacement perturbed from the steady state solution can be regarded as a disturbance entering the plant as shown in figure 4. The responses for the disturbance $\Delta\theta := \theta(0) - 9.296 \times 10^{-2} = -0.1$ rad perturbed from the steady state solution, can be computed using figure 2 are shown in figure 6. Note that the small deflection assumption is not violated since $v_{\max}(\ell,t)/\ell = \theta_{\max}(t) = 9.296\%$ (less than 10%).

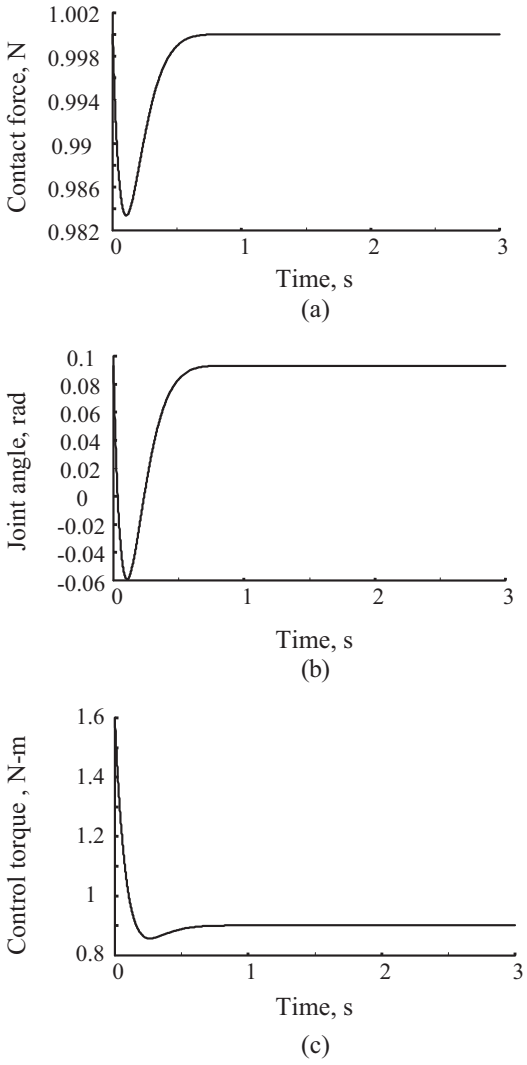

Fig. 6: Disturbance rejection: (a) $\lambda(t)$; (b) $\theta(t)$; (c) $\tau(t)$.

9 Conclusions and future work

In this paper, exact solutions of the noncollocated infinite-dimensional force control system has been obtained. With the joint torque as the input and the contact force as the output, the noncollocated system is confirmed as a non-minimum phase. Based on a new input from root bending moment and output redefinition via parallel compensation, a passive transfer function is erected for the noncollocated system. Particularly, necessary and sufficient conditions in the passivity properties are revealed for the first time in this field.

Besides, it is found that a passive PD controller suffices to stabilize the infinite-dimensional closed loop system. Unlike most traditional approaches based on truncated models, which will generally suffer from control and observation spillover problems. Simulations have verified that the proposed scheme can track the contact force promptly and accurately. One future research area is to relax the small deflection assumption so that a much larger contact force can be controlled.

Appendix

The infinite product expansions for transcendental functions used in this paper are summarized as follows [22,27]. In accordance with the context of this paper, $\hat{s}^2 = -\beta^4$ is used whenever it is appropriate.

A1. $\sin\beta + \sinh\beta = 2\beta \prod_{n=1}^{\infty} \left(1 - \frac{\hat{s}^2}{\omega_{zn}^2}\right)$, $\omega_{zn} = 2a_n^2$

$\tanh a_n + \tan a_n = 0, \quad (a_n > 0, \text{real})$

$a_n = \left(n - \frac{1}{4}\right)\pi$ as $n \to \infty$

$\omega_{z1} = 2(2.365)^2, \omega_{z2} = 2(5.498)^2, \omega_{z3} = 2(8.639)^2,$

$\omega_{z4}=2(11.781)^2, \omega_{z5}=2(14.923)^2, \omega_{z6}=2(18.064)^2$

A2. $\sin\beta\sinh\beta = \beta^2 \prod_{n=1}^{\infty} \left(1 + \frac{\hat{s}^2}{n^4\pi^4}\right)$

A3. $\cosh\beta\sin\beta - \cos\beta\sinh\beta = \frac{2}{3}\beta^3 \prod_{n=1}^{\infty} \left(1 + \frac{\hat{s}^2}{\omega_{\beta n}^2}\right)$,

$\omega_{\beta n} = c_n^2, \tanh c_n - \tan c_n = 0, (c_n > 0, \text{real})$

$c_n = \left(n + \frac{1}{4}\right)\pi$ as $n \to \infty$

$\omega_{\beta 1} = 3.927^2, \omega_{\beta 2} = 7.069^2, \omega_{\beta 3} = 10.210^2,$

$\omega_{\beta 4} = 13.352^2, \omega_{\beta 5} = 16.493^2, \omega_{\beta 6} = 19.635^2$

A4. $1 + \cosh\beta\cos\beta = 2\prod_{n=1}^{\infty} \left(1 + \frac{\hat{s}^2}{\omega_{pn}^2}\right)$, $\omega_{pn} = b_n^2$

$\cosh b_n \cos b_n + 1 = 0 (b_n > 0, \text{real})$

$b_n = (n - \frac{1}{2})\pi$ as $n \to \infty$

$\omega_{p1} = 1.875^2, \omega_{p2} = 4.694^2, \omega_{p3} = 7.855^2,$

$\omega_{p4} = 10.996^2, \omega_{p5} = 14.137^2, \omega_{p6} = 17.279^2$

Note that the asymptotic expressions are found very accurate (to three decimal places) since $n \geq 5$.

References

[1] B. C. Chiou and M. Shahinpoor, Dynamic stability analysis of a one-link force-controlled flexible manipulator, Journal of Robotic Systems, Vol.5, No.5. (1988), 443-451.

[2] B. C. Chiou and M. Shahinpoor, Dynamic stability analysis of a two-link force-controlled flexible manipulator, ASME Journal of Dynamic Systems, Measurement, and Control, Vol.112, No.4. (1990), 661-666.

[3] D. Li, Tip-contact Force control of one-link flexible manipulator: an inherent performance limitation, Proceedings of 1990 American Control Conference, San Diego, CA., (1990), 697-701.

[4] F. Matsuno, Y. Sakawa and T. Asano, Quasi-static hybrid position/force control of a flexible manipulator, Proceedings of 1991 IEEE International Conference on Robotics and Automation, Sacramento, CA., (1991), 2838-2842.

[5] F. Matsuno, T. Asano and Y. Sakawa, Quasi-static hybrid position/force control of constrained planar two-link flexible manipulators, IEEE Trans. Robotics and Automation, Vol.10, No.3. (1994), 287-297.

[6] A. Garcia and V. Feliu, Force control of a single-link flexible robot based on a collision detection mechanism, Proceedings of 2000 IEE Control Theory Appl., Vol.147, No.6. (2000), 588-595.

[7] I. Payo, V. Feliu and M. Moallem, Force control of a single-link flexible arm, IEEE 3rd International Conference on Mechatronics, Budapest, July 2006, pp.575-580.

[8] J. Becedas, I. Payo and V. Feliu, Generalised proportional integral torque control for single-link flexible manipulators, IET Control Theory Appl., Vol.4, No.5. (2010), 773-783.

[9] X. Ding and J. M. Selig, Dynamic modeling of a compliant arm with 6-dimensional tip forces using screw theory, Robotica, Vol.21, No.2. (2003), 193-197.

[10] O. Ma and J. Wang, Model order reduction for impact-contact dynamics simulations of flexible manipulators, Robotica, Vol.25, No.4. (2007), 397-407.

[11] J. Lin and T. S. Chiang, A new design of hierarchical fuzzy hybrid position/force control for flexible link robot arm, Proceedings of 2003 American Control Conference, Denver, Colorado, (2003), 5239-5244.

[12] J. Lin, Hierarchical fuzzy logic controller for a flexible link robot arm performing constrained motion tasks, Proceedings of 2003 IEE Control Theory Appl., Vol.150, No.4. (2003), 355-364.

[13] S. Kilicaslan, M. K. Ozgoren and S. K. Ider, Control of constrained spatial three-link flexible manipulators, 2007 Mediterranean Conference on Control and Automation, Athens-Greece, (2007), 1-6.

[14] F. Matsuno and S. Kasai, Modeling and robust force control of constrained one-link flexible arms, Journal of Robotic Systems, Vol.15, No.8. (1998), 447-464.

[15] A. Bazaei and M. Moallem, Force transmission through a structurally flexible beam: dynamic modeling and feedback control, IEEE Transactions on Control Systems Technology, Vol.17, No.6. (2009), 1245-1256.

[16] F. Matsuno, S. Umeyama and S. Kasai, Experimental study on robust force control of a flexible arm with a symmetric rigid tip body, Proceedings of 1997 IEEE International Conference on Robotics and Automation, Albuquerque, New Mexico, (1997), 3136-3141.

[17] Y. Morita, Y. Kobayashi, H. Kando, F. Matsuno, T. Kanzawa and H. Ukai, Robust force control of a flexible arm with a nonsymmetric rigid body, Journal of Robotic Systems, Vol.18, No.5. (2001), 221-235.

[18] A. Bazaei and M. Moallem, Improving force control bandwidth of flexible-link arms through output redefinition, IEEE/ASME Transactions on Mechatronics, Vol.16, No.2. (2011), 380-386.

[19] T. Endo and F. Matsuno, Dynamics based force control of one-link flexible arm, SICE 2004 Annual Conference, Sapporo, (2004), 2736-2741.
[20] Y. Morita, F. Matsuno, M. Ikeda, H. Ukai and H. Kando, Experimental study on PDS force control of a flexible arm considering bending and torsional deformation, 7^{th} International Workshop on Advanced Motion Control, Maribor, Slovenia, (2002), 408-413.
[21] M. Francis, C. Ching and D. Wang, Exact solution and infinite-dimensional stability analysis of a single flexible link in collision, IEEE Trans. Robotics and Automation, Vol.19, No.6. (2003), 1015-1020.
[22] L. Y. Liu and K. Yuan, "Force control of a constraint one-link flexible arm: a distributed parameter modeling approach, Journal of Chinese Institute of Engineers, Vol.6, No.4. (2003), 443-454.
[23] L. Y. Liu and H. C. Lin, PD control of a constrained flexible arm via parallel compensation, International Conference on Manufacturing and Engineering Systems, Taiwan, (2010), 276-281.
[24] K. Yuan and C. M. Hu, Nonlinear modeling and partial linearizing control of a slewing timoshenko-beam manipulator, ASME Journal of Dynamic Systems, Measurement, and Control, Vol.118, No.1. (1996), 75-83.
[25] K. Yuan, Control of slew maneuver of a flexible beam mounted non-radially on a rigid hub: a geometrically exact modelling approach, J. of Sound and Vibration, Vol.204. No. 5. (1997), 795-806.
[26] L. Qiu and E. J. Davison, Performance limitations of non-minimum phase systems in servomechanism problem, Automatica, Vol.29, No.2. (1993), 337-349.
[27] K. Yuan and L. Y. Liu, Achieving minimum phase transfer function for a noncollocated single-link flexible manipulator, Asian Journal of Control, Vol. 2, No. 3. (2000), 179-191.
[28] C. Trautman and D. Wang, Noncollocated passive control of a flexible link manipulator, Proceedings of 1996 IEEE International Conference on Robotics and Automation, Minneapolis, Minnesota, (1996), 1107-1114.
[29] H. Geniele, R. V. Potel and K. Khorasani, End-Point Control of a Flexible-Link Manipulator : Theory and Experiments, IEEE Transactions On Control Systems Technology, Vol.5, No.6. (1997), 556-570.
[30] D. Wang and M. Vidyasagar, Passive control of a stiff flexible link, International Journal of Robotic Research, Vol.11, No. 6. (1992), 572-578.
[31] J. C. Doyle, B. A. Francis and A. R. Tannenbaum, Feedback Control Theory (Macmillan, New York, 1992).

Liang-Yih Liu received his M.S. and Ph.D. degrees in mechanical engineering from National Taiwan University in 1994 and 2003, respectively. His current research interests include modeling and control of flexible manipulators.